Supplementary Information

Tube-like Pd@Coordination Polymer with Enhanced Solar Light Harvesting for Boosting Photocatalytic H_2 Production in A Wide pH Range and Seawater

Jieling Li,† Shihao Sun,† Ningshuang Gao, Hua Li, Kun Liang,* Jun Hai, Suisui He, Xijiao Mu,* Baodui Wang*

Key Laboratory of Nonferrous Metal Chemistry and Resources Utilization of Gansu Province, State Key Laboratory of Applied Organic Chemistry, College of Chemistry and Chemical Engineering, Lanzhou University, Lanzhou 730000, P. R. China

†These authors contributed equally to this work.

* Corresponding author.

E-mail: liangk@lzu.edu.cn; muxijiao@gmail.com; wangbd@lzu.edu.cn

1. Characterizations.

Field-emission scanning electron microscope (FE-SEM, FEI, Sirion 200), transmission electron microscope (TEM, Talos-200s), X-ray powder diffraction (XRD, AXS D8-Advanced diffractometer), X-ray photoelectron spectroscopy (XPS) measurements were investigated on a PHI-5702 multifunctional spectrometer using Al Kα radiation. Emission spectra were recorded on a Shimadzu RF-5301 spectrophotometer. characterize the morphology and composition of the material. FT-IR spectra were performed on a Nicolet FT-170SX spectrometer. Diffuse reflectance UV–Vis spectra of samples is analyzed by UV-vis diffuse reflectance spectra (DRS) with $BaSO_4$ as the reference by Shimadzu UV-1750 spectrophotometer. Steady-state fluorescence measurements were detected by Shimadzu RF-5301 spectrofluorometer with an excitation

wavelength of 380 nm. Fluorescence lifetimes were determined using the time-correlated single photon counting (TCSPC) mode. The sample was excited with a NanoLED-330 (Horiba) with an excitation wavelength of 380 nm.

2. DFT Calculation.

In this work, the conformational search is performed using the CREST[1] program combined with meta-dynamics and genetic algorithms.[2] GFN-FF performs first coarse conformational filtering, and then the GFN2-XTB[3] method is used for preferential selection. Finally, the B3LYP[4] functional and def2-TZVP[5] basis set are used to optimize the final structure. The ellipsoidal potential[6] is used in the protonation and deprotonation calculations to test the solution. The IR spectra are performed by B3LYP functional and 6-31++G* basis sets and the NMR spectra has calculated by MP2 with cc-pVDZ basis sets. Excited-state calculations are performed using the time-dependent density functional theory (TDDFT) method combined with CAM-B3LYP[7] general function and def2-TZVP basis set. The electron-hole pair analysis is implemented by Multiwfn 3.78 and plotted by VMD-1.9.3.9 The X-ray PES are performed by QTP17 functional10 and aug-cc-pVDZ basis sets[8].

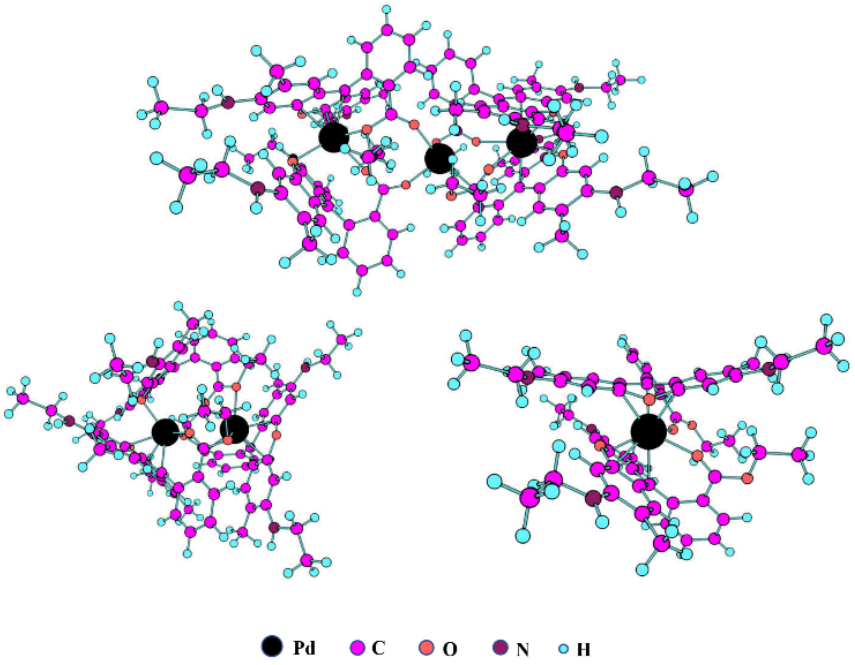

Figure S1. The calculated structure of Pd(II)CPs.

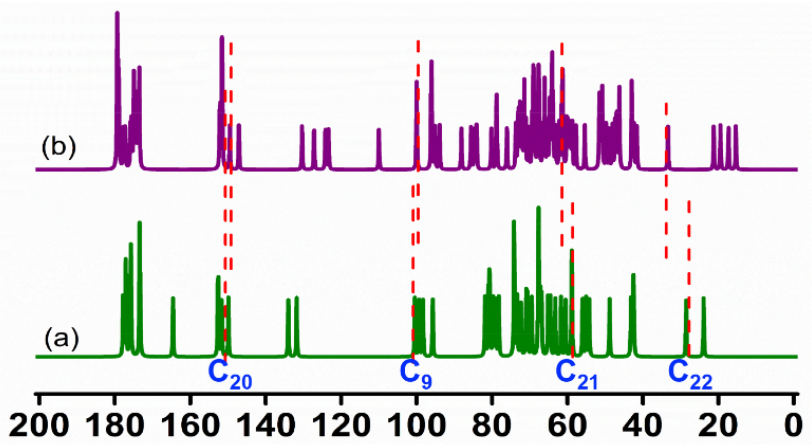

Figure S2. Calculated ^{13}C MAS NMR spectra: (a) Rh6G; (b) Pd(II)CPs.

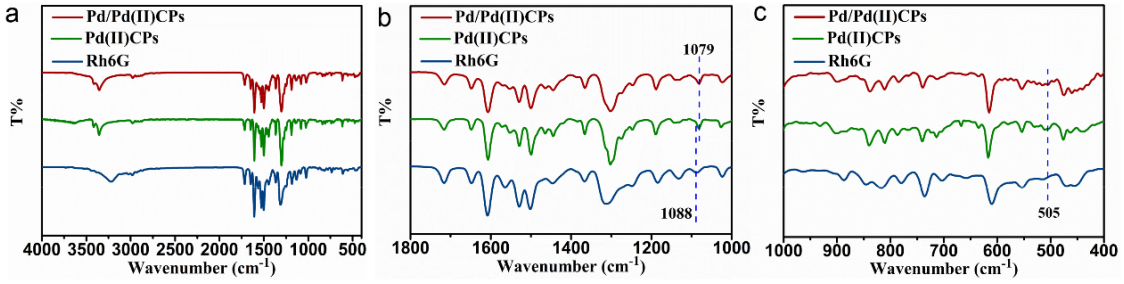

Figure S3. (a, b) FT-IR spectra and (c) magnified view of FT-IR spectra of Pd/Pd(II)CPs.

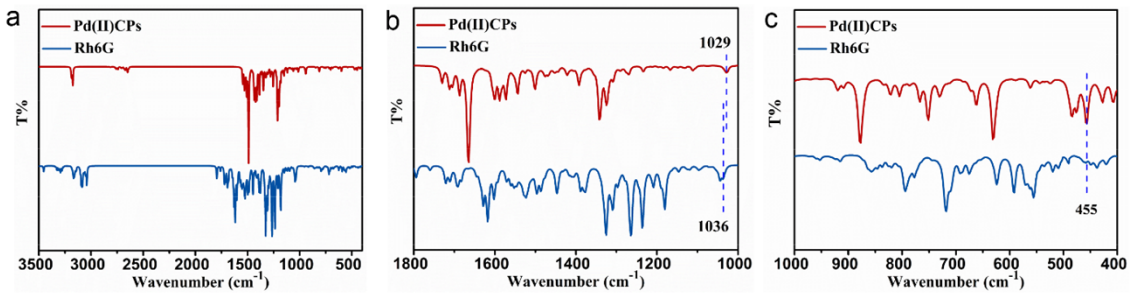

Figure S4. Calculated (a, b) FT-IR spectra and (c) magnified view of FT-IR spectra of Pd(II)CPs.

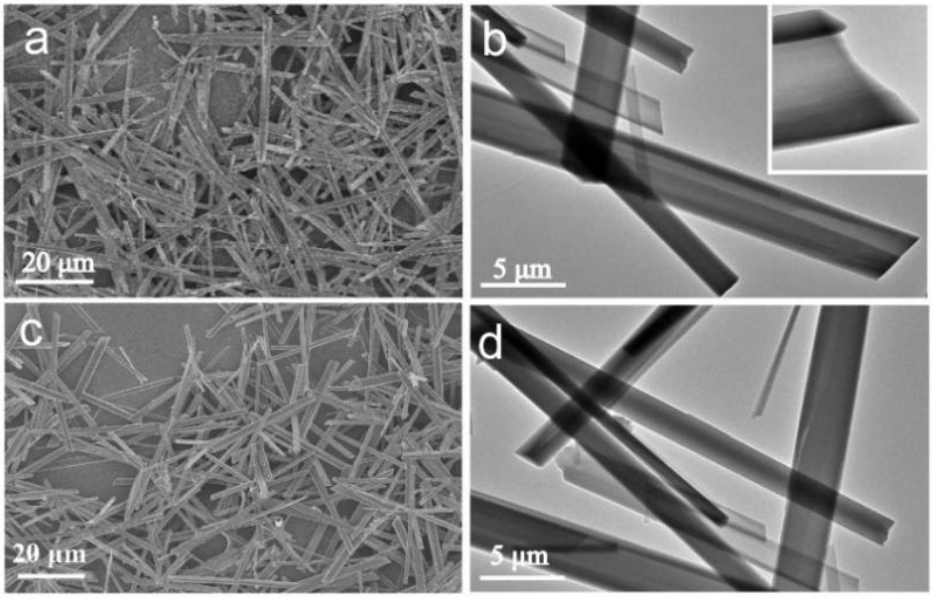

Figure S5. (a) SEM image and (b) TEM image of Pd(II)CPs. (c) SEM images and (d) TEM image of Pd/Pd(II)CPs.

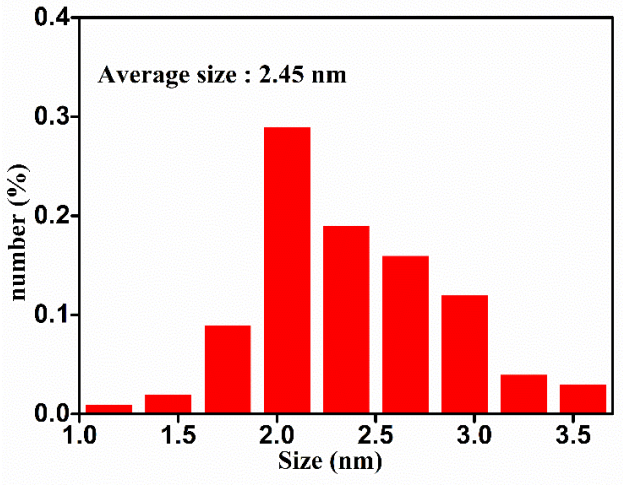

Figure S6. Size distribution of Pd nanoparticles encapsulated within Pd/Pd(II)CPs.

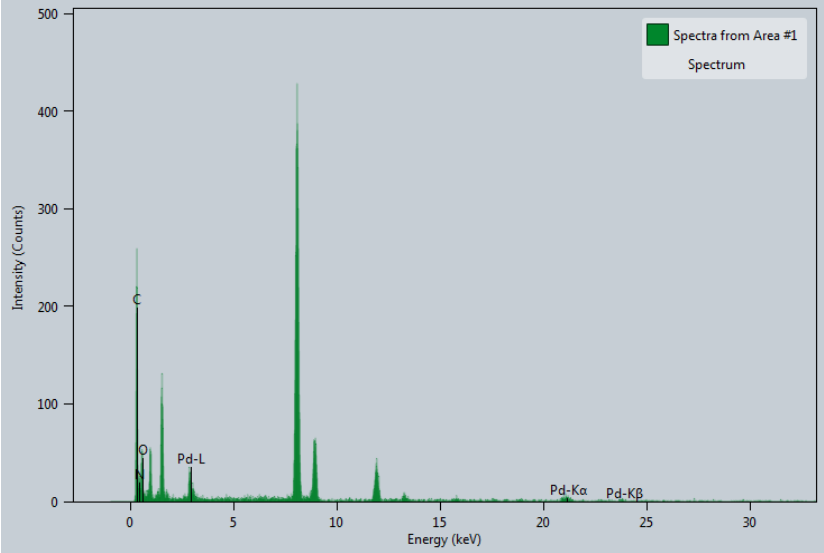

Figure S7. EDX spectrum of Pd/Pd(II)CPs.

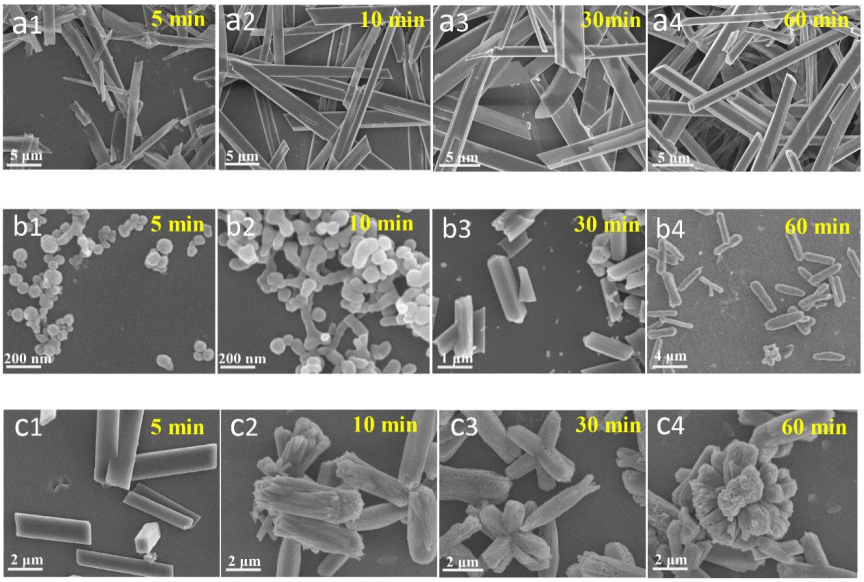

Figure S8. Time-dependent SEM image of Pd/Pd(II)CPs. SEM images of Pd/Pd(II)CPs fabricated under various conditions: ethanol/water with NaBr (a1-a4), water with NaBr (b1-b4), and water without NaBr (c1-c4).

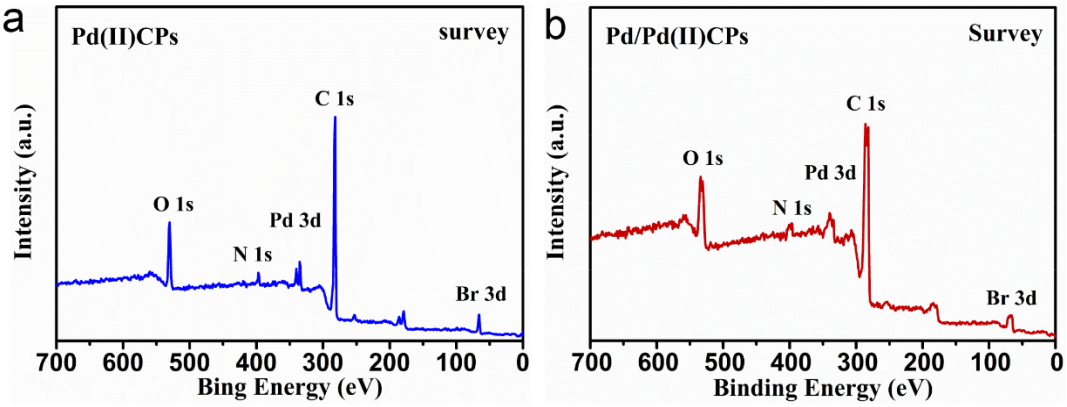

Figure S9. Survey XPS spectra of (a) Pd(II)CPs and (b) Pd/Pd(II)CPs.

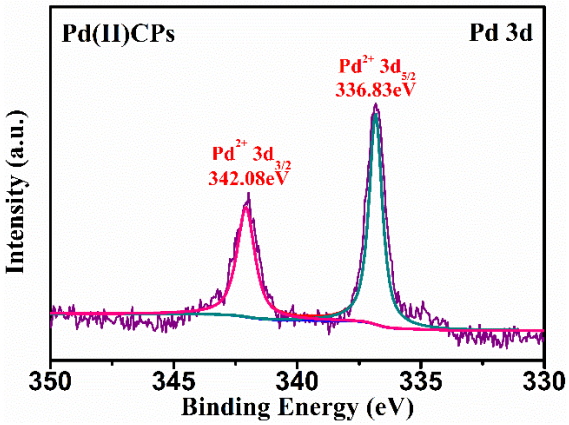

Figure S10. Pd 3d XPS spectra of Pd(II)CPs.

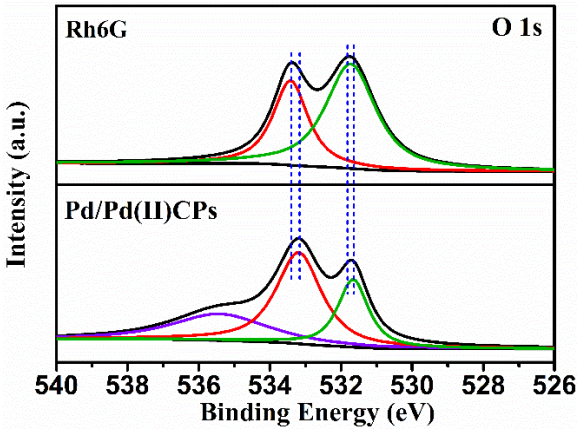

Figure S11. O 1s XPS spectra of Rh6G and Pd/Pd(II)CPs.

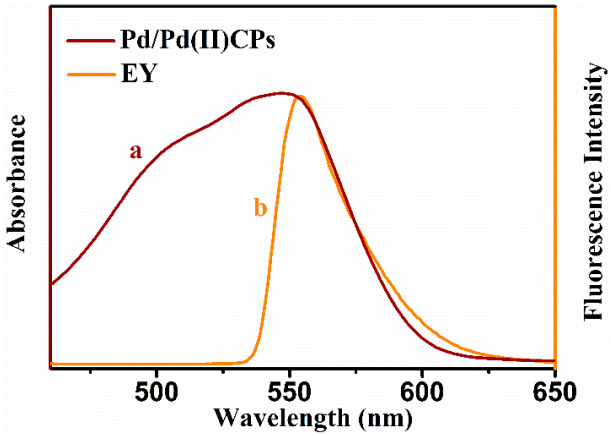

Figure S12. (a) UV−vis diffuse reflectance spectra, (b) luminescence spectral of EY upon excitation at 380 nm of Pd/Pd(II)CPs.

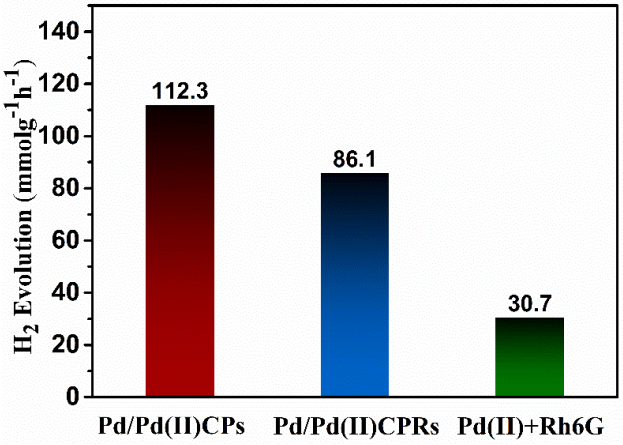

Figure S13. Photocatalytic hydrogen production on EY-sensitized Pd/Pd(II)CPs , Pd/Pd(II)CPRs , and Pd(II) iron mixed with Rh6G(500 mW cm^{-2}).

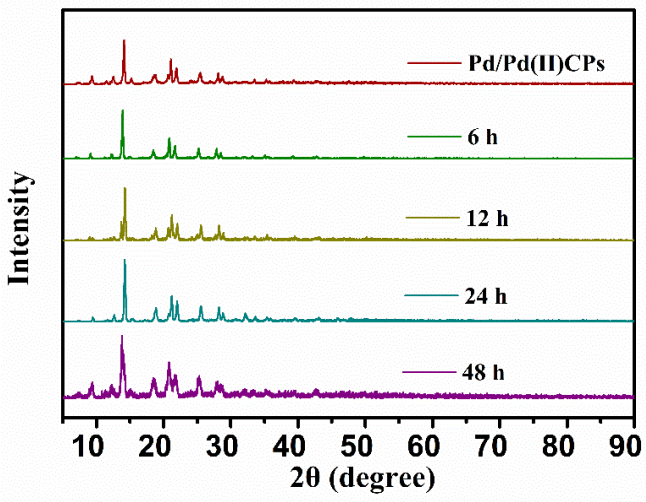

Figure S14. PXRD patterns of Pd/Pd(II)CPs after soaked in seawater of different hours.

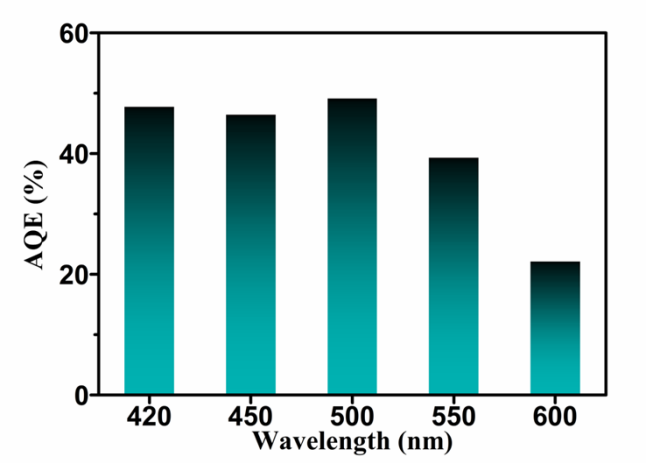

Figure S15. Wavelength-dependent apparent quantum efficiency (AQE) of H_2 evolution.

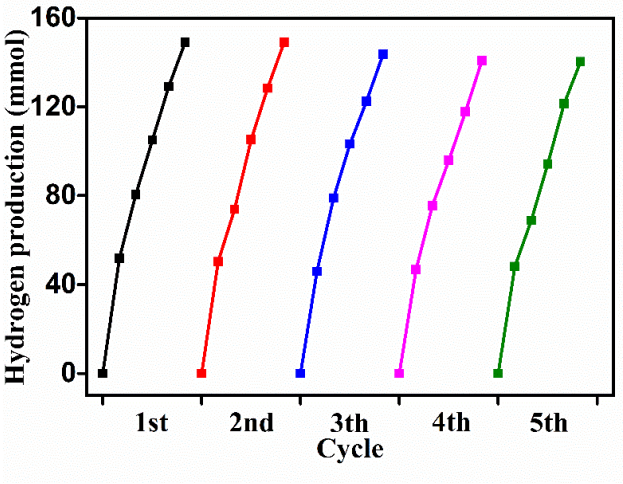

Figure S16. Cycling test (100 mW cm^{-2}) over Pd/Pd(II)CPs.

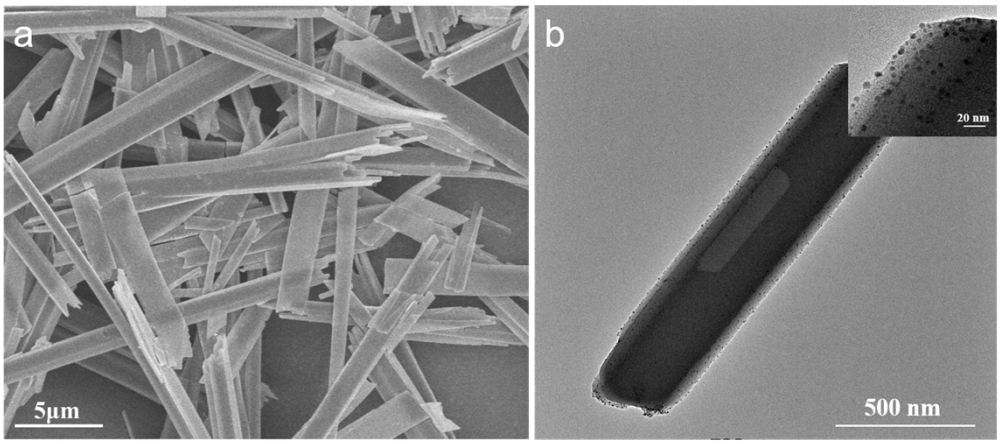

Figure S17. (a) SEM and (b) TEM image of Pd/Pd(II)CPs collected after five cycles.

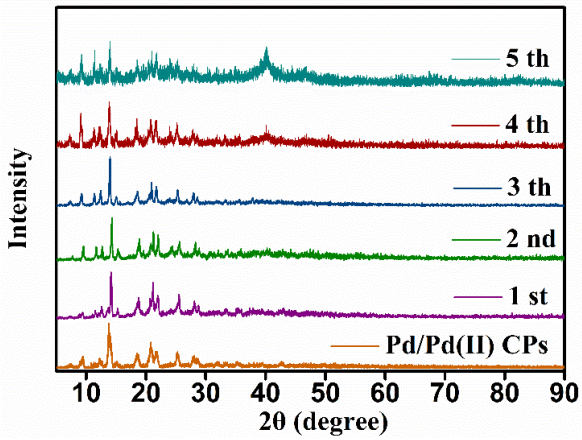

Figure S18. PXRD patterns of Pd/Pd(II)CPs collected from the reaction solution.

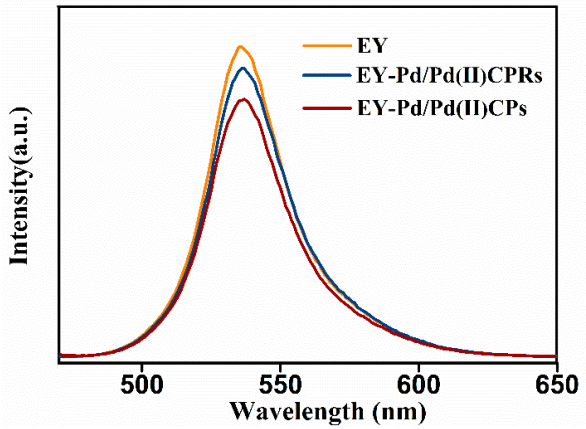

Figure S19. Steady-state PL emission spectra (λex=380 nm) of Pd/Pd(II)CPs and Pd/Pd(II)CPRs.

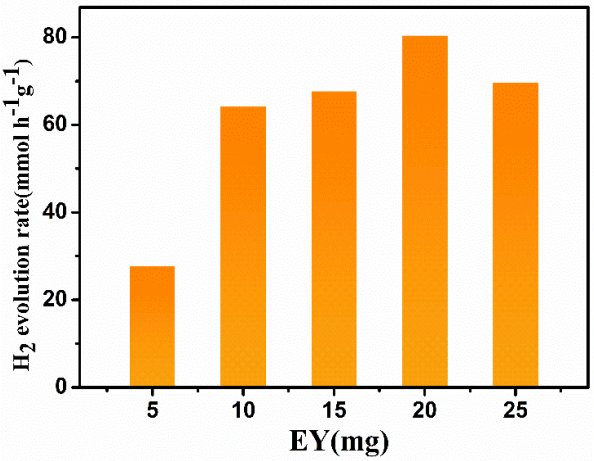

Figure S20. Photocatalytic hydrogen production performance of different amounts of EY.

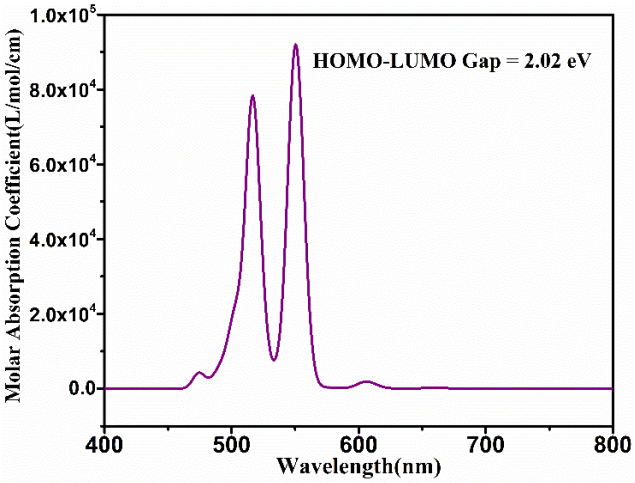

Figure S21. The theoretical absorption spectra of Pd(II)CPs calculated by TDDFT method based on the Pd(II)CPs structure searched by MTD-GC.

Table S1. Chemical shift changes of carbon on Rh6G and Pd/Pd(II)CPs.

Name	Chemical shift of Rh6G (ppm)	Chemical shift of Pd/Pd(II)CPs (ppm)	Difference (ppm)	Calculated chemical shift of Rh6G (ppm)	Calculated chemical shift of Pd/Pd(II)CPs (ppm)
C_{20}	166.7	165.7	-1.0	149.9	148.8
C_9	114.6	113.2	-1.4	101.2	99.6
C_{21}	59.4	62.2	2.8	58.5	61.6
C_{22}	13.6	16.2	2.6	27.8	33.9

Table S2. FT-IR spectra changes of Rh6G and Pd/Pd(II)CPs.

Name	Wavelength of Rh6G (cm^{-1})	Wavelength of Pd/Pd(II)CPs (cm^{-1})	Calculated wavelength of Rh6G (cm^{-1})	Calculated wavelength of Pd/Pd(II)CPs (cm^{-1})
C-O	1088	1079	1036	1029
Pd-O	0	505	0	455

Table S3. Performance comparison of different photocatalysts reported in literature.

Photocatalyst	H_2 production rate	Sacrificial agent	Light source	Ref.

	(μmol $h^{-1}g^{-1}$)			
EY-sensitized CuRSH	7880	10 vol% TEOA	λ≥420 nm	9
EY-sensitized NH_2-MIL-125(Ti)/0.75CN/$Ni_{15.8}$	53050	1 vol% TEOA	visible-light source	10
EY-sensitized MoS_2 QDs /UiO-66-NH_2/G	75.1	10 vol% TEOA	λ≥420 nm	11
EY-sensitized NiMo@MIL-10	740.2	10 vol% TEOA	λ≥420 nm	12
EY-sensitized Ni@MOF-5	30.22	10 vol% TEOA	λ≥420 nm	13
EY-sensitized Ag@Ag-Pd alloy	41.64	HCHO 0.75 mol/L	420 nm cut-off filter	14
EY-sensitized 1%Ni:Fe_3S_4	3260	10 vol% TEOA	visible light (>420 nm)	15
EY-sensitized 1%Pt:Fe_3S_4	2256	10 vol% TEOA	visible light (>420 nm)	15
EY-sensitized MIL-53(Fe)	315	10 vol% TEOA	300W Xe lamp 100 mW cm^{-2}	16
Pt-doped PdTAPP–TFPT gel	1970	sodium ascorbate	λ>420 nm	17
$Pd_{0.75}/TiO_2$	53640	25 vol% methanol	300W Xe lamp 200 mW cm^{-2}	18
Pd_{SA+C}/TiO_2-V_O	18196.6	methanol aqueous solution (20 vol%)	365 nm	19
Pd/CoP@CoNiP superstructures	3845	10 vol% TEOA	300W Xe lamp 250-900 nm	20
EY-sensitized Pd/Pd(II)CPs.	112340	8 vol% TEOA	300W Xe lamp 400-780 nm	**This work**
EY-sensitized Pd/Pd(II)CPRs.	86730	8 vol% TEOA	300W Xe lamp 400-780 nm	**This work**

References

1. P. Pracht, F. Bohle and S. Grimme, *Phys Chem Chem Phys*, 2020, **22**, 7169-7192.
2. C. Bannwarth, S. Ehlert and S. Grimme, *J Chem Theory Comput,* 2019, **15**, 1652-1671.

3. A. D. Becke, *Phys Rev A Gen Phys,* 1988, **38**, 3098-3100.
4. B. P. Pritchard, D. Altarawy, B. Didier, T. D. Gibson and T. L. Windus, *J Chem Inf Model,* 2019, **59**, 4814-4820.
5. E. P. Pokatilov, V. M. Fomin, J. T. Devreese, S. N. Balaban and S. N. Klimin, *Physica E: Low-dimensional Systems and Nanostructures,* 1999, **4**, 156-169.
6. T. Yanai, D. P. Tew and N. C. Handy, *Chemical Physics Letters,* 2004, **393**, 51-57.
7. T. Lu and F. Chen, *J Comput Chem,* 2012, **33**, 580-592.
8. W. Humphrey, A. Dalke and K. Schulten, *Journal of Molecular Graphics,* 1996, **14**, 33-38.
9. X. Y. Dong, M. Zhang, R. B. Pei, Q. Wang, D. H. Wei, S. Q. Zang, Y. T. Fan and T. C. Mak, *Angew. Chem. Int. Ed.,* 2016, **55**, 2073-2077.
10. J. Xu, J. Gao, C. Wang, Y. Yang and L. Wang, *Appl. Catal. B-Environ.,* 2017, **219**, 101-108.
11. X. Hao, Z. Jin, H. Yang, G. Lu and Y. Bi, *Appl. Catal. B-Environ.,* 2017, **210**, 45-56.
12. W. Zhen, H. Gao, B. Tian, J. Ma and G. Lu, *ACS Appl. Mater. Inter,* 2016, **8**, 10808-10819.
13. W. Zhen, J. Ma and G. Lu, *Appl. Catal. B-Environ.,* 2016, **190**, 12-25.
14. H. Liu, M. Wang, X. Zhang, J. Ma and G. Lu, *Appl. Catal. B-Environ.,* 2018, **237**, 563-573.
15. M. Zhang, X. Chen, X. Jiang, J. Wang, L. Xu, J. Qiu, W. Lu, D. Chen and Z. Li, *ACS Appl. Mater. Inter,* 2021, **13**, 14198-14206.
16. S. Li, F. Wu, R. Lin, J. Wang, C. Li, Z. Li, J. Jiang and Y. Xiong, *Chem. Eng. J.,* 2022, **429**, 132217.
17. P. Liao, Y. Hu, Z. Liang, J. Zhang, H. Yang, L.-Q. He, Y.-X. Tong, J.-M. Liu, L. Chen and C.-Y. Su, *J. Mater. Chem. A,* 2018, **6,** 3195-3201.
18. T. Lv, B. Xiao, F. Xia, M. Chen, J. Zhao, Y. Ma, J. Wu, J. Zhang, Y. Zhang and Q. Liu, *Chem. Eng. J.*, 2022, **450**, 137873.
19. T. Wang, X. Tao, X. Li, K. Zhang, S. Liu and B. Li, *Small,* 2021, **17**, e2006255.
20. B. Fang, Z. Xing, W. Kong, Z. Li and W. Zhou, *Nano Energy*, 2022, **101**, 107616.